Available online at www.sciencedirect.com
SCIENCE DIRECT®
Journal of Sound and Vibration 269 (2004) 113–133
JOURNAL OF SOUND AND VIBRATION
www.elsevier.com/locate/jsvi

Design of a broadband active silencer using μ-synthesis

Mingsian R. Bai*, Pingshun Zeung

Department of Mechanical Engineering, National Chiao-Tung University, 1001 Ta-Hsueh Road, Hsin-Chu 30010, Taiwan, Republic of China

Received 5 June 2002; accepted 19 December 2002

Abstract

A robust spatially feedforward controller is developed for broadband attenuation of noise in ducts. To meet the requirements of robust performance and robust stability in the presence of plant uncertainties, a μ-synthesis procedure via D–K iteration is exploited to obtain the optimal controller. This approach considers uncertainties as modelling errors of the nominal plant in high frequency and is implemented using a floating point digital signal processor (DSP). Experimental investigation was undertaken on a finite-length duct to justify the proposed controller. The μ- controller is compared to other control algorithms such as the H_2 method, the H_∞ method and the filtered-U least mean square (FULMS) algorithm. Experimental results indicate that the proposed system has attained 25.8 dB maximal attenuation in the band 250–650 Hz.

1. Introduction

Compared to conventional passive technologies, active noise control (ANC) offers numerous advantages, e.g., compact size and low-frequency performance. Fixed controllers based on optimal control and robust control are gaining research attention in the field of ANC, even the adaptive feedforward controllers, e.g., the least mean square (LMS) method and its variants are being widely used [1–5]. Many design techniques have been applied to the duct ANC problem for synthesizing fixed controllers. Hong et al. [6] and Wu et al. [7] investigated the duct ANC problem using the linear quadratic Gaussian (LQG) control. Along the same line, robust controllers are designed using combined pole placement and loop shaping method [8]. Bai and Wu [9] solved the problem via linear programming in the l_1- and l_2-norm vector space using model matching approach. In an earlier research, Bai and Chen [10] developed the H_2 and H_∞ model matching principle to deal with the same problem. To suppress narrowband noise, an internal model-based

*Corresponding author. Tel.: +886-3-5720634.
E-mail address: msbai@cc.nctu.edu.tw (M.R. Bai).

0022-460X/03/$ - see front matter
doi:10.1016/S0022-460X(03)00006-3

ANC system has also been proposed by Hu [11]. In the work of Bai and Lin [12], H_∞ robust control theory was used to compare three control structures: feedback control, feedforward control, and hybrid control in terms of performance, stability, and robustness.

In ANC applications to date, feedforward control has been the most effective approach. However, a non-acoustical reference required by feedforward control is usually unavailable in many applications. The *spatially feedforward* control structure shown in Fig. 1(a) appears to be the only approach in dealing with such situations, especially when broadband attenuation is sought. The term, spatially feedforward structure, stems from the fact that the ANC system in Fig. 1(b) includes an acoustic feedback path and is thus not a purely feedforward structure. In this case, stability and robustness problems will arise and the achievable performance will also be degraded. In addition, the perturbation between the nominal plants and real plants should be considered in designing the ANC controller. Common causes of plant uncertainties are modelling errors, measurement noises, and the perturbations in physical conditions. A comprehensive investigation on the effect of different physical conditions on ducts such as flow, temperature, lining, and radiation impedance, can be found in Ref. [13]. However, in this paper, we shall focus on primarily the uncertainties resulting from modelling errors on which the robust control design is based.

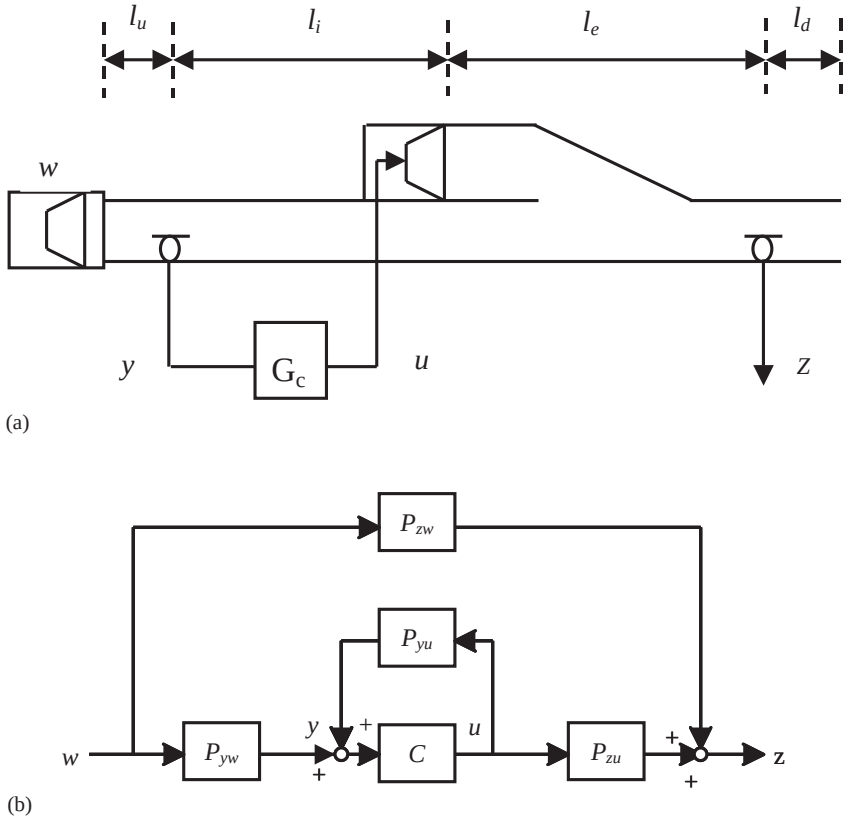

Fig. 1. The spatially feedforward structure; (a) the ANC system of a duct and (b) the equivalent block diagram.

A control method ensuring robust stability and robust performance is highly desirable. Therefore, the μ-synthesis control is proposed for the design of a spatially feedforward controller for duct ANC problems. Two interconnected structures for modelling the ANC system are used to develop the controllers. The first structure does not account for uncertainty, while the second structure does. Thus, the controller synthesized via the H_2 method or the H_∞ method in the first case focuses its effort on nominal performance. However, when the H_∞ method is used to design the controller under the second structure considering uncertainty, the control performance is reduced and tends to be conservative. Then, μ-synthesized controller is introduced in the second case and obtains good noise reduction which is comparable to the performance of the H_∞ method in the first structure. In an experimental verification using a finite-length duct, the aforementioned fixed controllers are also compared to the filtered-U least mean square (FULMS) controller which is a widely used method in dealing with feedforward ANC problem.

2. μ-synthesis control design

The objective of robust control is to achieve acceptable performance for all models within a specified, bounded uncertainty set. In comparison with the other control strategies, μ-synthesis provides a design procedure with the ability to cope with the stringent requirement of robust performance. In this section, the general ideas of μ-synthesis will be given, alongside a brief review of the H_∞ control theory for it is the basis of the former theory.

2.1. H_∞ Control theories

All control structures, including the feedback and the feedforward structures could be cast into a generalized control framework in robust control theory. The framework, as illustrated in Fig. 2(a), contains a controller $\mathbf{K}(s)$ and an *augmented plant* $\mathbf{P}(s)$ where $\mathbf{z}(t)$ is a vector signal including all controlled signals and tracking errors, $\mathbf{w}(t)$ is a vector signal including noise, disturbances, and reference signal, $\mathbf{u}(t)$ is the control signal, and $\mathbf{y}(t)$ is the measurement output. The relationships between these variables are described as

$$\begin{bmatrix}\mathbf{Z}(s)\\ \mathbf{Y}(s)\end{bmatrix} = \mathbf{P}(s)\begin{bmatrix}\mathbf{W}(s)\\ \mathbf{U}(s)\end{bmatrix} = \begin{bmatrix}\mathbf{P}_{11}(s) & \mathbf{P}_{12}(s)\\ \mathbf{P}_{21}(s) & \mathbf{P}_{22}(s)\end{bmatrix}\begin{bmatrix}\mathbf{W}(s)\\ \mathbf{U}(s)\end{bmatrix},$$
$$\mathbf{U}(s) = \mathbf{K}(s)\mathbf{Y}(s), \tag{1}$$

where the submatrices $\mathbf{P}_{ij}(s)$ are compatible partitions of the augmented plant $\mathbf{P}(s)$.

The objective of the H_∞ control is to minimize the infinity norm of the transfer function matrix from $\mathbf{W}(s)$ to $\mathbf{Z}(s)$, which is denoted by $\mathbf{T}_{zw}(s)$ that can be expressed by lower *linear fraction transformation* (LFT):

$$\mathbf{T}_{zw}(s) = F_l(\mathbf{P},\mathbf{K}) = \mathbf{P}_{11}(s) + \mathbf{P}_{12}(s)\mathbf{K}(s)[\mathbf{I} - \mathbf{P}_{22}(s)\mathbf{K}(s)]^{-1}\mathbf{P}_{21}(s). \tag{2}$$

The mathematical statement of the H_∞ control problem is then represented as

$$\min_{k(s)} \|\mathbf{T}_{zw}(s)\|_\infty = \min_{k(s)} \sup_{-\infty \leqslant \omega \leqslant \infty} \bar{\sigma}[\mathbf{T}_{zw}(j\omega)]. \tag{3}$$

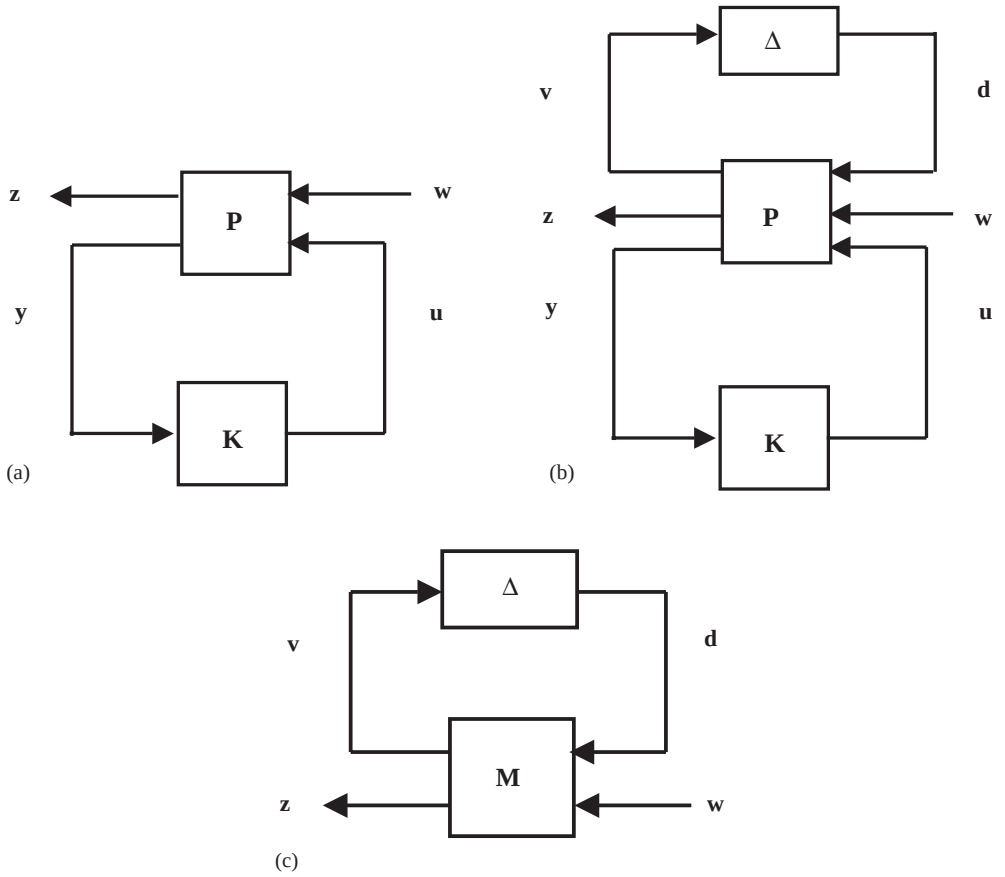

Fig. 2. Block diagrams of robust control structure: (a) generalized control framework in robust control theory, (b) generalized framework in μ-synthesis control theory and (c) linear fractional transformation with an uncertainty model.

However, an optimal H_∞ controller is generally very difficult to find. In practice, it is usually easier to obtain a "suboptimal" controller using the γ-iteration [14]. In other words, we are content with finding a stabilizing controller such that

$$\|\mathbf{T}_{zw}(s)\|_\infty < \gamma. \tag{4}$$

The details of the synthesis procedure involving the solutions of two Riccati equations can be found in Refs. [15,16] and are omitted here for simplicity.

2.2. μ-Analysis

Because the H_∞ controller is conservative in structured uncertainty model, the μ-synthesis controller is introduced to provide better performance. The general framework used in μ-synthesis controller design is shown in Fig. 2(b). The interconnected structure incorporates an *augmented plant* $\mathbf{P}(s)$, a controller $\mathbf{K}(s)$ and an uncertainty set $\mathbf{\Delta}(s)$ into one large system where $\mathbf{v}(t)$ and $\mathbf{d}(t)$ correspond to model uncertainties or perturbations while $\mathbf{z}(t)$, $\mathbf{w}(t)$, $\mathbf{u}(t)$, and $\mathbf{y}(t)$ have been

defined as Fig. 2(a). The closed-loop transfer function $\mathbf{M}$ shown in Fig. 2 (c) is derived as a lower LFT $\mathbf{M} = F_l(\mathbf{P}, \mathbf{K}) = \mathbf{P}_{11} + \mathbf{P}_{12}\mathbf{K}(\mathbf{I} - \mathbf{P}_{22}\mathbf{K})^{-1}\mathbf{P}_{21}$ defined in Eq. (2).

Furthermore, the transfer function from $\mathbf{w}(t)$ to $\mathbf{z}(t)$ is represented as an upper LFT

$$\mathbf{z} = F_u(\mathbf{M}, \mathbf{\Delta})\mathbf{w}, \tag{5}$$

where

$$F_u(\mathbf{M}, \mathbf{\Delta}) = \mathbf{M}_{22}(s) + \mathbf{M}_{21}(s)\mathbf{\Delta}(s)(\mathbf{I} - \mathbf{M}_{11}(s)\mathbf{\Delta}(s))^{-1}\mathbf{M}_{12}(s),$$

$$\mathbf{M} = \begin{bmatrix} \mathbf{M}_{11} & \mathbf{M}_{12} \\ \mathbf{M}_{21} & \mathbf{M}_{22} \end{bmatrix}.$$

The uncertainty model $\mathbf{\Delta}$ is assumed to belong to the set

$$\mathbf{\Delta} = \left\{ diag\left(\delta_1 \mathbf{I}_{k_1}, \ldots, \delta_r \mathbf{I}_{k_r}, \mathbf{\Delta}_1, \mathbf{\Delta}_2, \ldots, \mathbf{\Delta}_S\right) : \delta_i \in C, \mathbf{\Delta}_j \in C^{m_j \times m_i} \right\}, \tag{6}$$

$$B\mathbf{\Delta} = \{\mathbf{\Delta} \in \mathbf{\Delta} | \bar{\sigma}(\mathbf{\Delta}) \leqslant 1\}, \tag{7}$$

where $\delta_i \mathbf{I}_{k_r}$ denotes *blocks-repeated scalar* uncertainty and $\mathbf{\Delta}_j$ denotes *full* block uncertainty. Two non-negative integers, r and s, represent the number of repeated scalar blocks and the number of full blocks, respectively. The dimension of the ith repeated scalar block is $k_i \times k_i$, while the jth full block is $m_j \times m_i$ [17]. In Eq. (7), $\bar{\sigma}$ indicates the maximum singular value.

In the design of H_∞ controller, robustness to unstructured uncertainty is considered, using an infinity norm test on $\mathbf{M}_{11}$. Unstructured uncertainty corresponds to the perturbation $\mathbf{\Delta}$ as a single full block. Unfortunately, norm bounds are inadequate for dealing with robust performance or realistic descriptions of plant uncertainty. The *structured singular value* μ, which is a generalization of a singular value, is used to analyze the robust stability and robust performance for a system with structured uncertainty. For a system $\mathbf{M}$, the *structured singular value* μ is defined as [18]

$$\mu_\Delta(\mathbf{M}) = \left(\min_{\Delta \in \Delta} \{\bar{\sigma}(\mathbf{\Delta}) : \det(\mathbf{I} - \mathbf{\Delta}\mathbf{M}) = 0\} \right)^{-1}, \tag{8}$$

which is essentially a measure of the smallest uncertainty $\mathbf{\Delta}$ that may distabilize the closed-loop system.

By setting the model uncertainty $\mathbf{\Delta}$ in the problem formulation to zero in Fig. 2(c), we get that nominal performance is just a norm test on $\mathbf{M}_{22}$, i.e.,

$$\|\mathbf{M}_{22}\|_\infty = \sup_w \bar{\sigma}[\mathbf{M}_{22}(s)]. \tag{9}$$

μ introduced in the above is used in the following two theorems [18], characterizing two properties of a system with structured uncertainties.

Theorem 1 (Robust stability). *The linear fractional transformation of the closed-loop system and the perturbation structure* $F_u(\mathbf{M}, \mathbf{\Delta})$, *is stable for all* $\mathbf{\Delta}$ *if and only if* $\mu(\mathbf{M}_{11}(s))$ *is less than* 1.

This theorem indicates that stability of any linear, time-invariant system in the presence of structured uncertainty can be rewritten as a structured singular value test.

Theorem 2 (Robust performance). *The linear fractional transformation of the closed-loop system and the perturbation structure* $F_u(\mathbf{M},\mathbf{\Delta})$, *is stable for all* $\mathbf{\Delta}$ *and* $\|F_u(\mathbf{M},\mathbf{\Delta})\|_\infty \leqslant 1$, *if and only if* $\sup_w \mu(\mathbf{M}(s))$ *is less than* 1.

This theorem implies that given a performance objective described in terms of an infinity norm test, robust performance of any linear, time-invariant system in the presence of structured uncertainty can be written as a structured singular value test.

2.3. μ-Synthesis

The ultimate goal of μ-synthesis is to find a stabilizing controller $\mathbf{K}(s)$ such that the transfer function from $\mathbf{w}(t)$ to $\mathbf{z}(t)$ has norm less than 1 in Fig. 2(b). In other words, the controller $\mathbf{K}(s)$ is synthesized to achieve the *robust performance*, which implies that the performance specifications of the closed-loop system are met for all uncertainty models. The objective of μ-synthesis could be represented as in the following equation:

$$\min_{\substack{K \\ stablizing}} \max_{\omega} \mu_\Delta[F_l(\mathbf{P},\mathbf{K})(j\omega)]. \tag{10}$$

Because there is no analytical solution available to the above problem, one generally employs a practical approach called *D–K iteration* technique [14,18]. This approach replaces $\mu_\Delta(\mathbf{M})$ by the upper bound for μ, $\bar{\sigma}\left[\mathbf{D}F_l(\mathbf{P},\mathbf{K})\mathbf{D}^{-1}\right]$, where $\mathbf{D}(s)$ is a stable, minimum phase transfer function with the form

$$\mathbf{D}(s) = \{diag[d_1\mathbf{I}, d_2\mathbf{I}, \ldots\ldots, d_{F-1}\mathbf{I}, \mathbf{I}] : d_i > 0\}. \tag{11}$$

The first procedure of *D–K iteration* is holding the scaling function $\mathbf{D}(s)$ fixed. After replacing the original interconnected structure $\mathbf{P}(s)$ with a new $\mathbf{P}_{scaled}(s)$ shown in Fig. 3, the following optimization is performed:

$$\min_{\substack{K \\ stablizing}} \left|\left|\mathbf{D}F_l(\mathbf{P},\mathbf{K})\mathbf{D}^{-1}\right|\right|_\infty, \tag{12}$$

which is the same as

$$\min_{\substack{K \\ stablizing}} \|F_l(\mathbf{P}_{scaled},\mathbf{K})\|_\infty. \tag{13}$$

Eq. (13) is an H_∞-optimization problem.

The next procedure is holding the controller $\mathbf{K}(s)$ fixed. The resulting scaling function $\mathbf{D}(s)$ is a function of frequency and is obtained by solving the following minimization corresponding to the

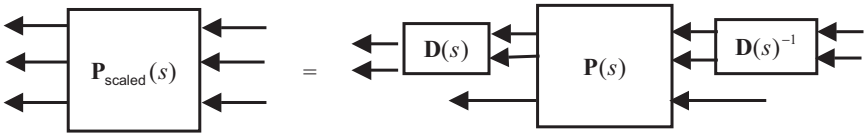

Fig. 3. Absorbing D scaling into open-loop interconnection.

upper bound for μ:

$$\min_{D} \bar{\sigma}[\mathbf{D}F_l(\mathbf{P},\mathbf{K})\mathbf{D}^{-1}], \tag{14}$$

which is a μ-analysis problem. Note that the scaling function $\mathbf{D}(s)$ typically contains some states, so the realization of the new $\mathbf{P}(s)$, $\mathbf{P}_{scaled}(s)$, usually has a higher state-space dimension than the original. Therefore, one need not approximate the $\mathbf{D}(s)$ function too accurately in the non-critical frequency ranges. Iterating the above two procedures, either the new H_∞-optimal $\mathbf{K}(s)$ is found to satisfy the μ-analysis objective or a new $\mathbf{D}(s)$ can be obtained. After iterations, the value $\bar{\mu}(\mathbf{M})$ will decrease and asymptotically converge to a certain value. The design is regarded as acceptable if the value is less than unity. In general, it takes only a few iterations to reach a suboptimal solution. The iteration is not guaranteed to reach the global minimum for the reason that both optimizations over $\mathbf{D}(s)$ and $\mathbf{K}(s)$ are convex, but the combined problem however is not necessarily convex. The details of μ analysis and synthesis can be found in Ref. [17].

3. μ-Synthesis of a duct ANC system

In the robust control design for duct ANC problems, it is assumed that a frequency-domain multiplicative type of uncertainty is used, i.e.,

$$P_{physical}(s) = P_{nominal}(s)[1 + \Delta(s)], \tag{15}$$

where $P_{physical}(s)$ represents the physical plant, $P_{nominal}(s)$ is the nominal plant, and $\Delta(s)$ is the multiplicative uncertainty [19]. The uncertainty considered here is primarily the difference between the plant model and the real plant beyond the control bandwidth, which may cause excessive control output at high frequency. Therefore, it is important for the controller to be robust against this type of uncertainty.

The general input–output relation of the augmented plant in Eq. (1) can be redefined as follows:

$$\begin{bmatrix} z(t) \\ y(t) \end{bmatrix} = \begin{bmatrix} P_{zw}(s) & P_{zu}(s) \\ P_{yw}(s) & P_{yu}(s) \end{bmatrix} \begin{bmatrix} w(t) \\ u(t) \end{bmatrix}, \tag{16}$$

where $P_{yu}(s)$, $P_{zu}(s)$, $P_{zw}(s)$, and $P_{yw}(s)$ are properly partitioned transfer functions of augmented plant $\mathbf{P}$ and they are shown in Fig. 1(b). To calculate the uncertainty defined in Eq. (15) for the duct ANC problem, four frequency responses of the partitioned plants are measured by a signal analyzer in 0–800 Hz and are regarded as the nominal plants, whereas four frequency responses measured in 0–1600 Hz are regarded as the physical plants.

Then, the frequency response magnitudes measured in 0–800 and in 0–1600 Hz as shown in Figs. 4 and 5, respectively, can be used to calculate the uncertainty of aforementioned four partitioned transfer functions of the augmented plant $\mathbf{P}$. The uncertainty $\Delta_i(s)$ of each transfer function is assumed to be bounded by a highpass weighting function $W_{high,i}(s)$, $i = 1, 2, 3, 4$. Based on the definition in Eq. (15), the weighting function $W_{high,i}(s)$ is selected according to the following equation:

$$\left| \frac{P_{physical}(j\omega)}{P_{nominal}(j\omega)} - 1 \right| \leqslant \left| W_{high,i}(j\omega) \right| \quad \forall\omega, \tag{17}$$

Fig. 6 shows the calculated uncertainty bounded by the chosen weighting function $W_{high,i}(s)$ of these four transfer functions, respectively. Note that we do not include the low-frequency part (below 250 Hz) in the measured frequency response during system identification for its poor coherence. In addition, the ripples in those diagrams of uncertainty below 650 Hz are due to the numerical errors in system identification. Thus, only the high-frequency part is important and these ripples are disregarded.

Two interconnected structures are illustrated here. The first structure does not consider the effect of uncertainty. Two synthesis methods, the H_∞ control and H_2 control are implemented in this structure. On the other hand, H_∞ control and μ-synthesis are applied in the second interconnected structure with uncertainty taken into consideration. The input–output relation of

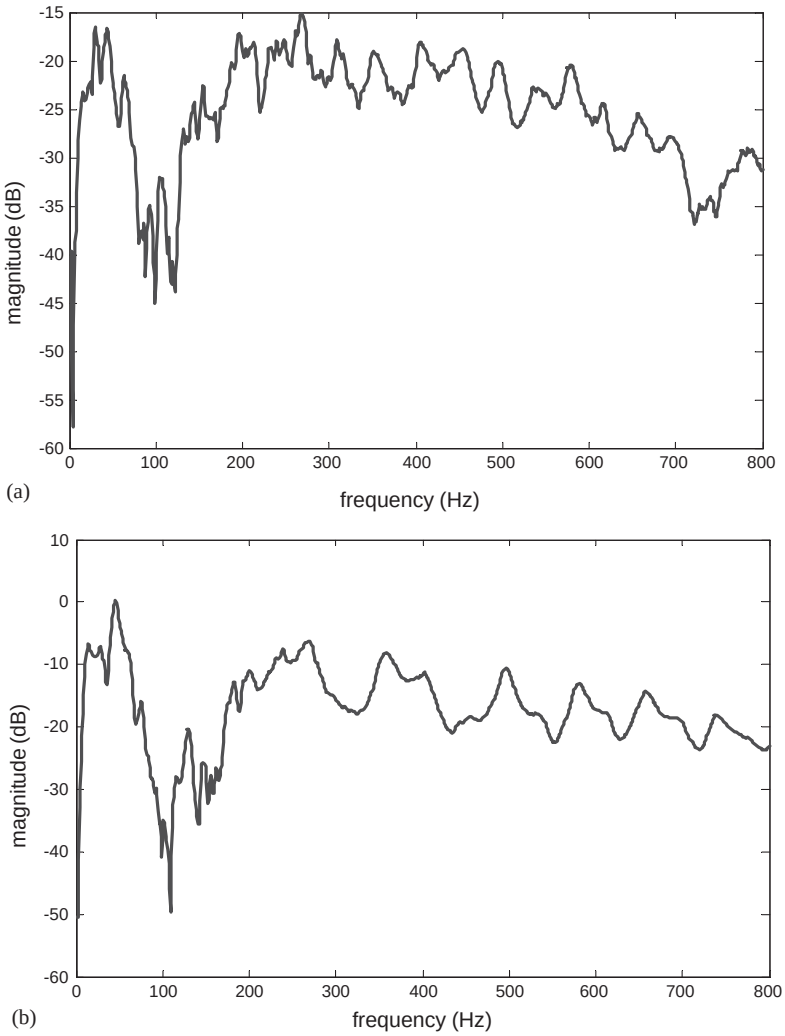

Fig. 4. The frequency responses of the nominal plants measured within 0–800 Hz: (a) P_{zw}; (b) P_{yw}; (c) P_{zu}; (d) P_{yu}.

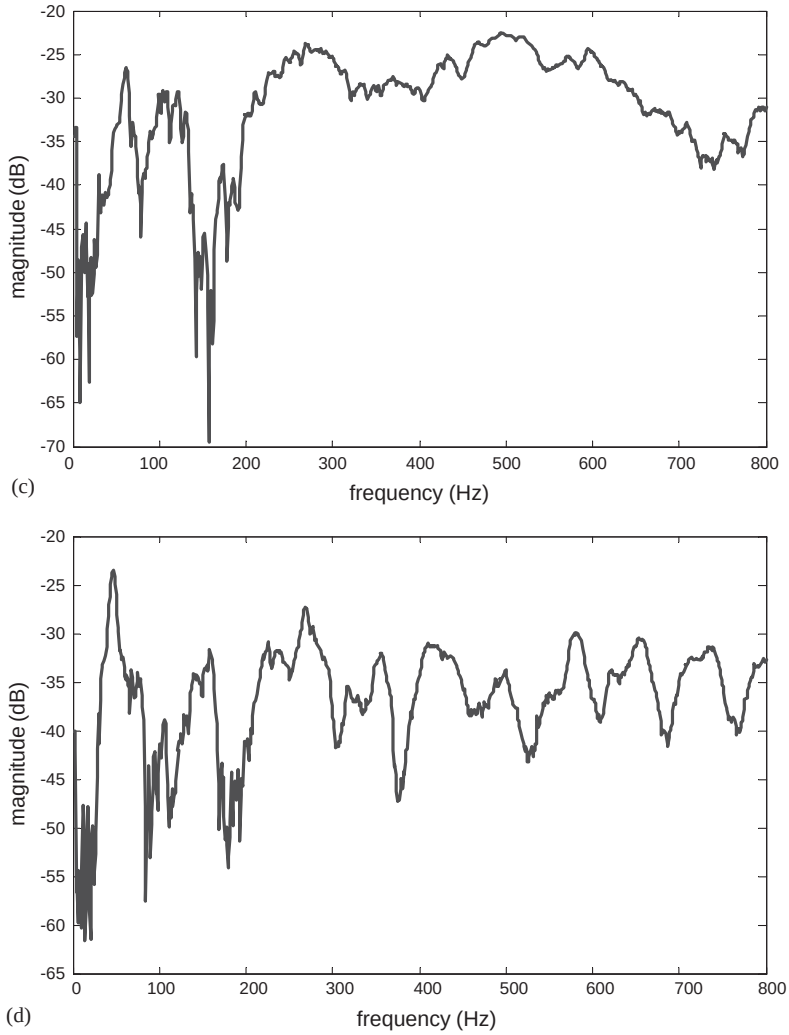

Fig. 4 (*continued*).

the augmented matrix corresponding to the first structure shown in Fig. 7 is described as follows:

$$\begin{bmatrix} z_1 \\ z_2 \\ y \end{bmatrix} = \mathbf{P} \begin{bmatrix} w \\ u \end{bmatrix} = \begin{bmatrix} W_b P_{zw} & W_b P_{zu} \\ 0 & W_{bs} \\ P_{yw} & P_{yu} \end{bmatrix} \begin{bmatrix} w \\ u \end{bmatrix}, \tag{18}$$

where W_b and W_{bs} are chosen to be bandpass and bandstop weighting functions, respectively. The term W_b is a performance weight for disturbance rejection in the desired frequency band. To prevent the system from instablility, controller weight W_{bs} is used to restrict the controller gain out of controlled frequencies. The second interconnected structure considering uncertainty is shown in Fig. 8. The block diagram of the duct system can be rearranged into the μ-synthesis framework in Fig. 2(b). The augmented plant $\mathbf{P}(s)$ used to synthesize the controller has vector

inputs and outputs arranged as follows:

$$\begin{bmatrix} v_1 \\ v_2 \\ v_3 \\ v_4 \\ v_5 \\ z \\ y \end{bmatrix} = \mathbf{P} \begin{bmatrix} d_1 \\ d_2 \\ d_3 \\ d_4 \\ w \\ u \end{bmatrix} = \begin{bmatrix} 0 & 0 & 0 & 0 & W_{high1} & 0 \\ 0 & 0 & 0 & 0 & W_{high2} & 0 \\ 0 & 0 & 0 & 0 & 0 & W_{high3} \\ 0 & 0 & 0 & 0 & 0 & W_{high4} \\ 0 & 0 & 0 & 0 & 0 & W_{bs} \\ W_b P_{zw} & 0 & W_b P_{zu} & 0 & W_b P_{zw} & W_b P_{zu} \\ 0 & P_{yw} & 0 & P_{yu} & P_{yw} & P_{yu} \end{bmatrix} \begin{bmatrix} d_1 \\ d_2 \\ d_3 \\ d_4 \\ w \\ u \end{bmatrix}. \tag{19}$$

The weighting functions of the above equation have been defined before.

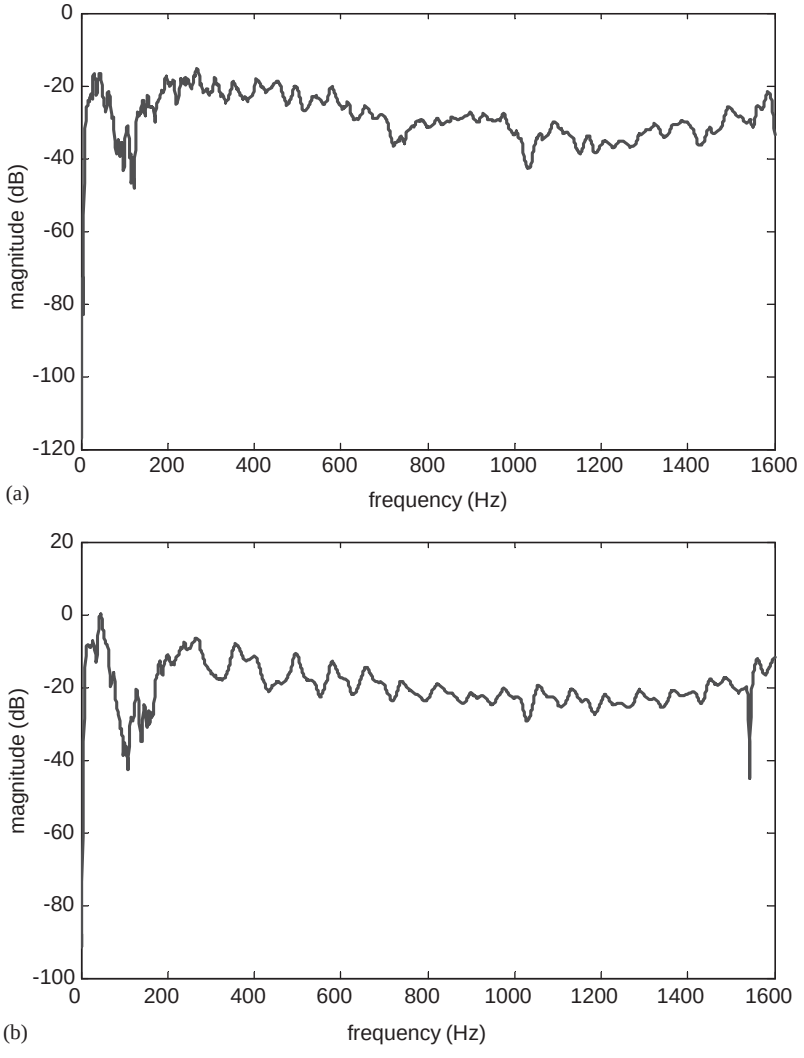

Fig. 5. The frequency responses of the real plants measured within 0–1600 Hz: (a) P_{zw}; (b) P_{yw}; (c) P_{zu}; (d) P_{yu}.

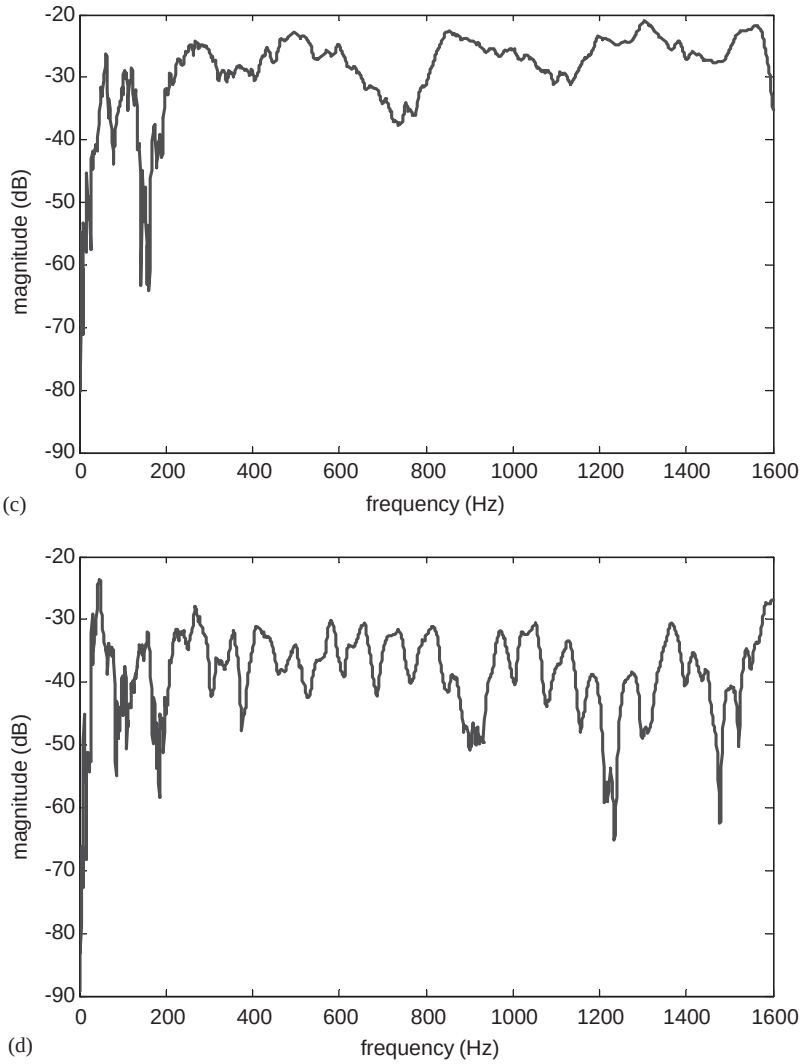

Fig. 5 (*continued*).

4. Experimental investigations

4.1. Experimental description

The experimental set-up in the spatially feedforward structure of a duct is shown in Fig. 9. A duct made of plywood is used for verifying the proposed ANC method. The length of the duct is 440 cm and the cross-section is 25 cm × 25 cm. The distance between the primary source speaker and the measurement microphone is 10 cm. To reduce acoustic feedback, we use the backward control loudspeaker facing the open end of the duct. The distance between the measurement

microphone and the control speaker is 100 cm to ensure causality of the controller. The distance between the control speaker and the performance microphone is 110 cm.

Two loudspeakers with 10 cm × 10 cm plane diaphragms are used to transmit primary (noise) and secondary (control) sources. The disturbance noise source is generated by a signal analyzer and the noise signal is picked up by the upstream sensor which is a unidirectional condenser microphone. Next, the noise signal is filtered by the controller implemented on the platform of a floating-point TMS320C32 digital signal processor (DSP) to generate the control source. The downstream microphone is used to monitor the control performance.

The DSP equipped with four 16-bit analog IO channels is utilized to implement different controllers. The sampling frequency is chosen to be 2 kHz. Considering the cut-off frequency of

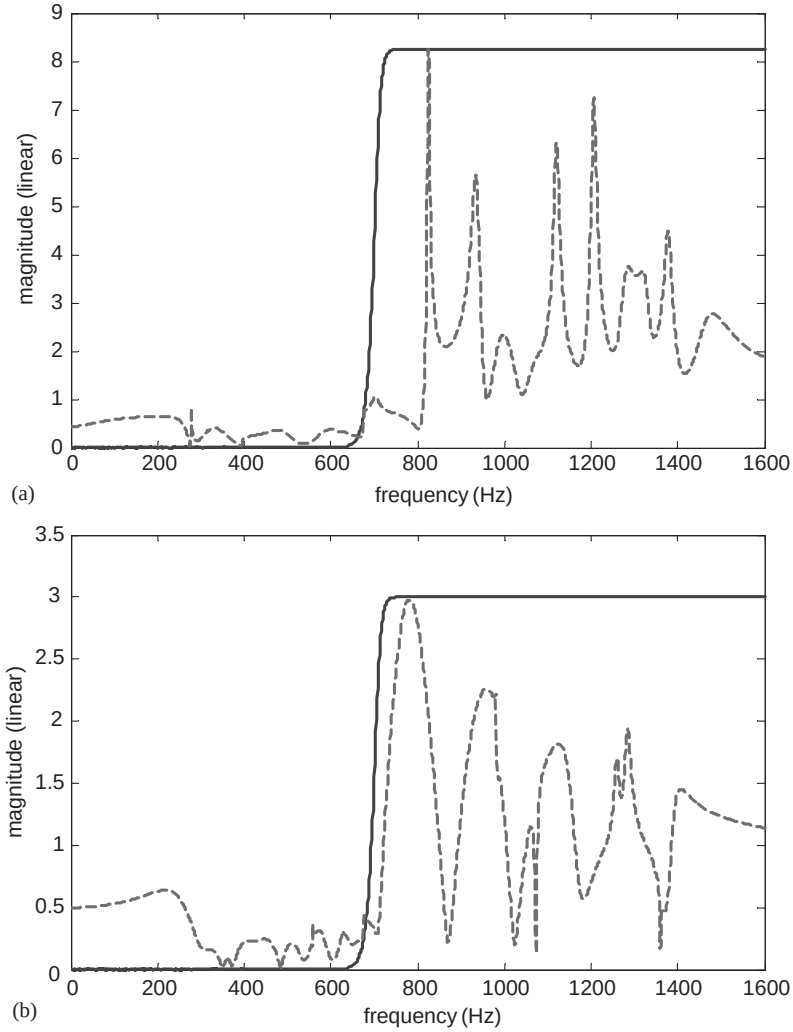

Fig. 6. Uncertainty and weighting functions. The results calculated for (a) P_{zw}; (b) P_{yw}; (c) P_{zu}; (d) P_{yu}.

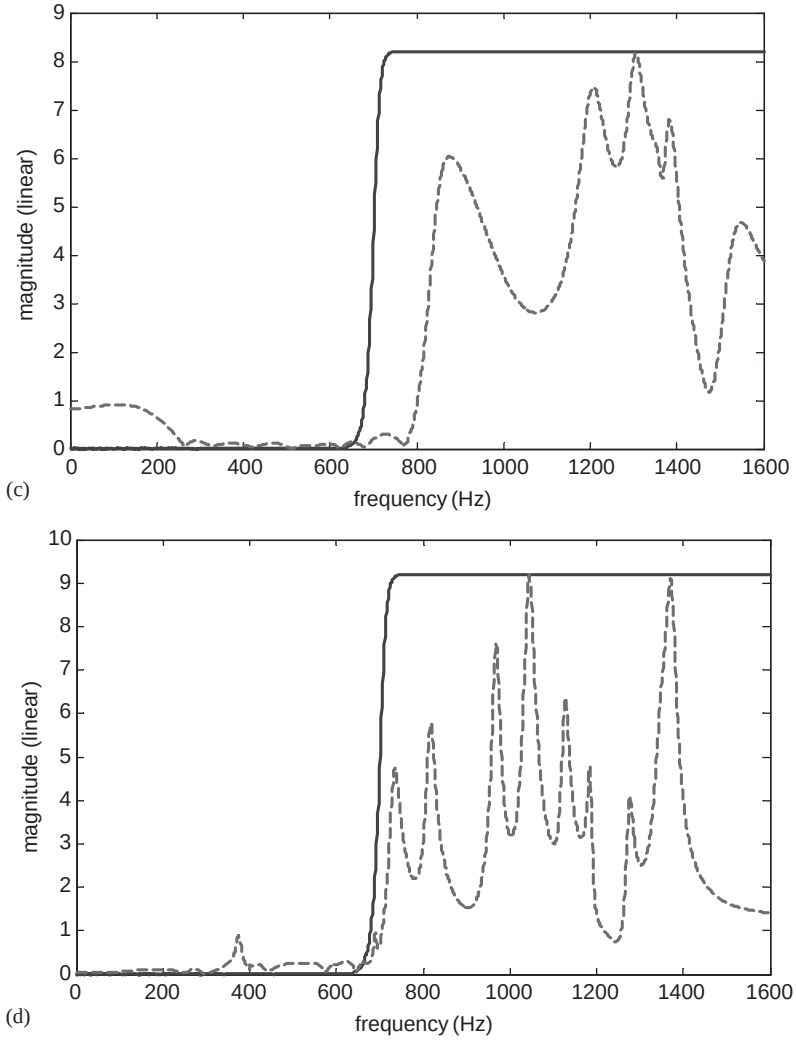

Fig. 6 (*continued*).

the duct (approximately 700 Hz) and the poor response of the speaker at low frequency, we chose control bandwidth from 250 to 650 Hz.

4.2. Experimental results

Two categories of experiments were performed for comparison. The H_∞ control and H_2 control are implemented in the structure shown in Fig. 7, which does not consider the effect of uncertainty, while the H_∞ control and μ-synthesis are applied in the second interconnected structure shown in Fig. 8, which takes uncertainty into consideration.

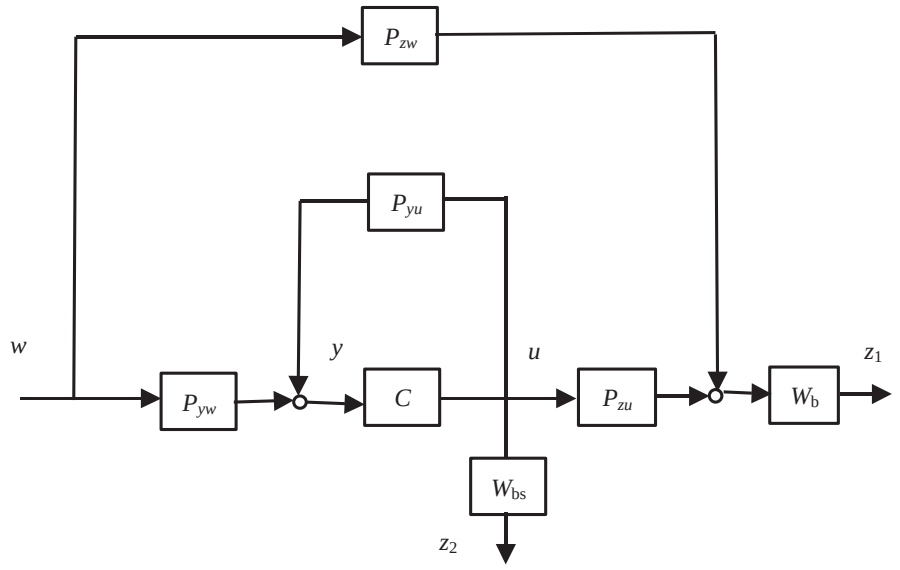

Fig. 7. The interconnected structure without considering uncertainty.

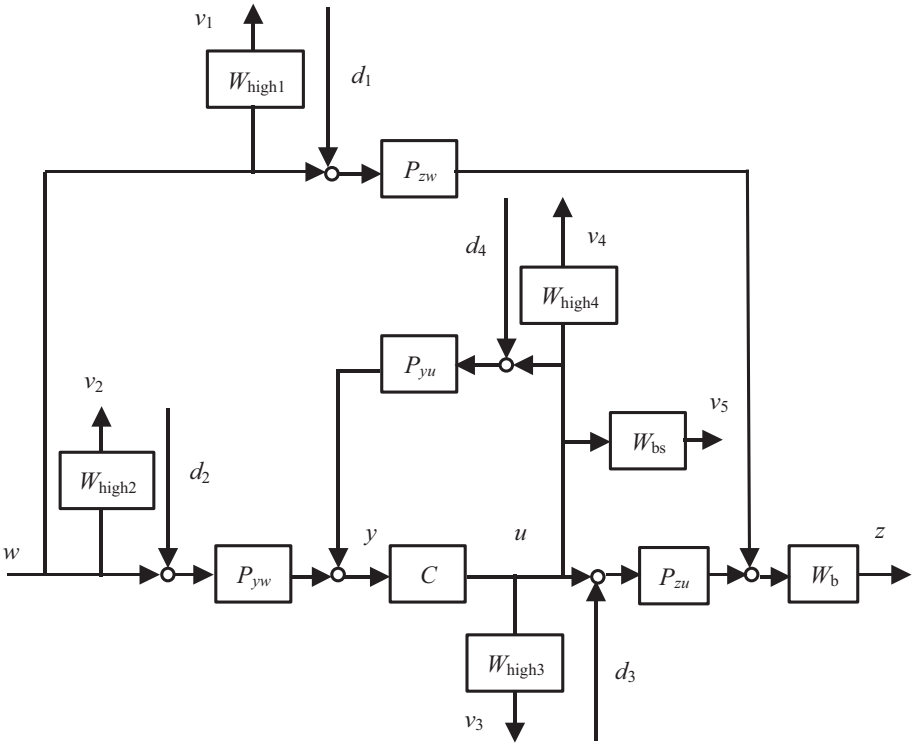

Fig. 8. The interconnected structure considering uncertainty.

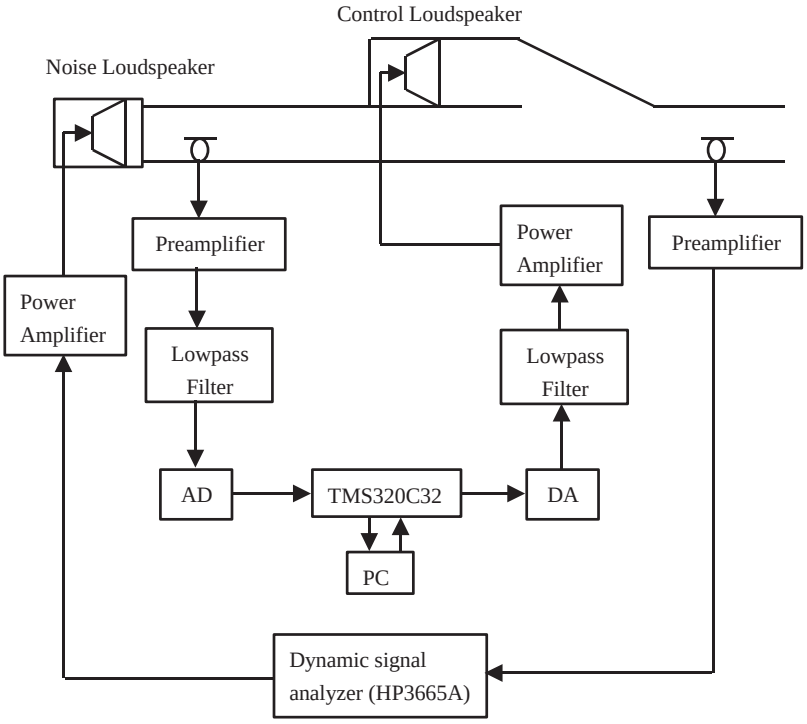

Fig. 9. Experimental set-up of the ANC problem.

The design procedures of the H_∞ and H_2 controllers for the structure in Fig. 7 are presented as follows. The gains of W_b and W_{bs} in Eq. (18) are chosen to be 25 and 27, respectively. To establish the augmented plant matrix in Eq. (18), the frequency responses of the partitioned transfer functions mentioned in Eq. (16) are identified via the Matlab command *invfreqz* [20]. These identified transfer functions are transformed from discrete- to continuous-time domain through *d2 cm* command because the μ-toolbox of Matlab [17] is used in s-domain. Next, model reduction is applied via a Matlab command, *sysbal* [17], to remove the unimportant and unnecessary dynamics. Then, Matlab commands, *h2syn* and *hinfsyn* [17], are introduced to obtain the H_2 and the H_∞ controllers, respectively. Because the orders of the controllers obtained are usually very high, model reduction is needed. After implementations on the platform of DSP with filter length 256, their performances are found to be very similar and the results of the H_2 and the H_∞ controllers are represented in Figs. 10(a) and (b). The total noise attenuation in the control bandwidth for H_2 controller is 7.17 dB while it is 6.77 dB for H_∞ controller. Because of the lack of uncertainty consideration, we achieved good performance. However, the controller synthesized in this structure cannot guarantee the robust stability and robust performance.

Now, we consider the control structure in Fig. 8, with uncertainty taken into account. After developing the augmented plant matrix in Eq. (19) and applying model reduction, H_∞ controller is synthesized and implemented again. Due to the conservative property of H_∞ control, the result shown in Fig. 11 is not as good as the case in Fig. 10(b) and the total noise attenuation is 4.37 dB.

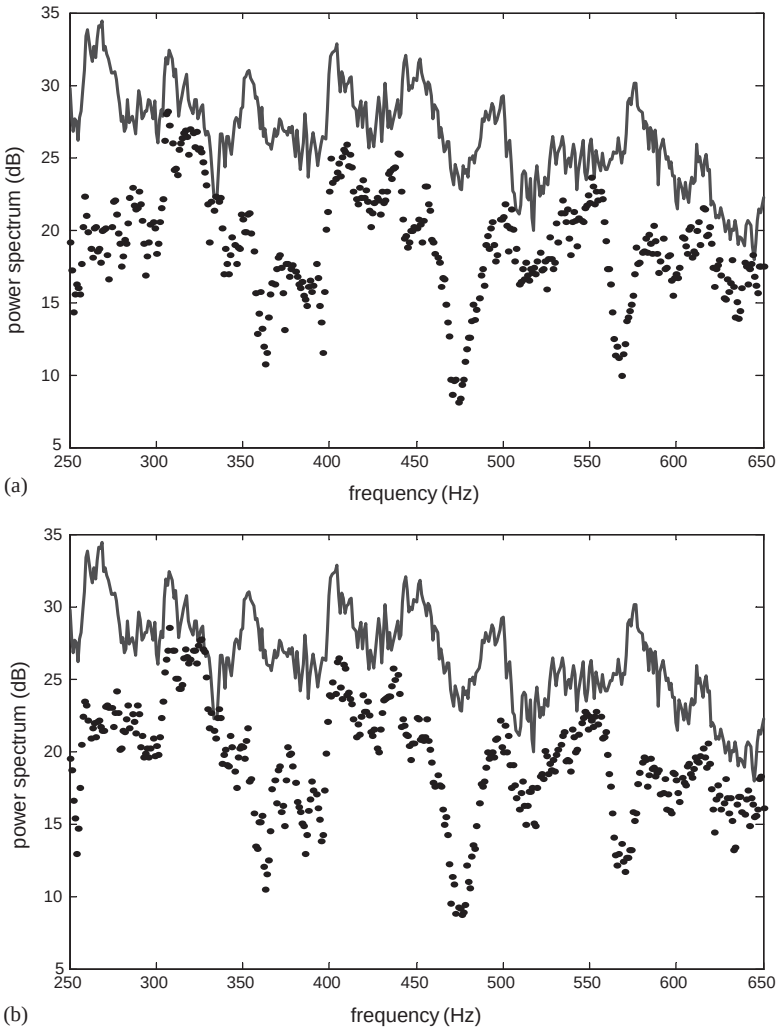

Fig. 10. Active control results of the feedforward controllers for interconnected structure in Fig. 7. Noise reduction using (a) H_2 controller; (b) H_∞ controller. ——, control off; ……, control on.

Thus, μ-synthesis control is applied to improve the performance. However, according to Theorem 1 in Section 2.2, the control system achieved robust stability.

First, the types of uncertainty blocks must be specified. In our case, the full complex block is chosen to be

$$\mathbf{\Delta} := \{ \begin{bmatrix} \mathbf{\Delta}_1 & 0 \\ 0 & \mathbf{\Delta}_2 \end{bmatrix} : \mathbf{\Delta}_1 = \begin{bmatrix} \Delta_{11} & 0 & 0 & 0 \\ 0 & \Delta_{12} & 0 & 0 \\ 0 & 0 & \Delta_{13} & 0 \\ 0 & 0 & 0 & \Delta_{14} \end{bmatrix}, \Delta_{11} \sim \Delta_{14} \in C^{1\times 1}, \mathbf{\Delta}_2 \in C^{1\times 2} \}, \tag{20}$$

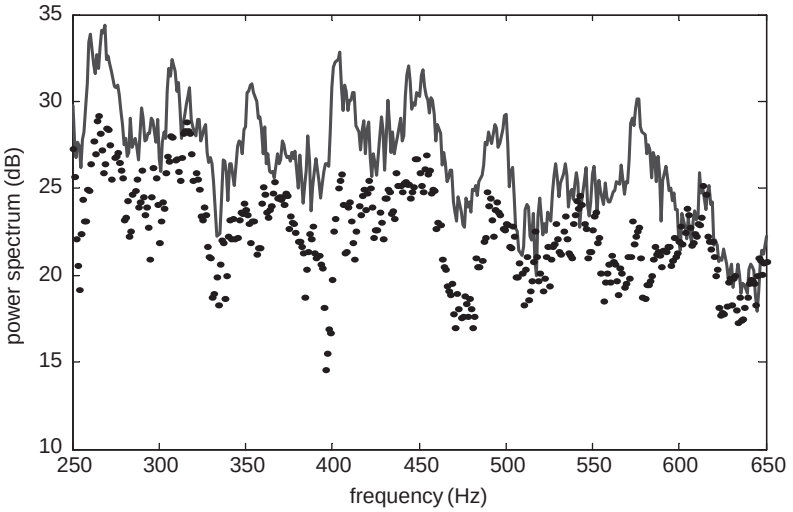

Fig. 11. Noise reduction using H_∞ controller for interconnected structure in Fig. 8. ——, control off; ……, control on.

where $\mathbf{\Delta}_1$ corresponds to the multiplicative uncertainty in Eq. (15) and $\mathbf{\Delta}_2$ is a fictitious uncertainty block to incorporate the performance objectives on the weighted output sensitivity transfer function into the μ-framework. Second, perform a μ-analysis of the closed-loop system obtained from the previous H_∞ control by the Matlab command *mu* [17]. The bounds for the structured singular value are shown in Fig. 12(a). In this μ-plot, there are many peaks within control bandwidth greater than 1. Hence, robust performance is not achieved according to Theorem 2 in Section 2.2. The objective is to make those peaks as small as possible to acquire larger bounds on allowable perturbation.

Then, another Matlab command *musynfit* is used to get **D** scaling matrix in the *D–K* iteration procedures. Next, we can merge the **D** matrix and original open-loop interconnection to form the new augmented plant for *hinfsyn* [17]. There are two facts noteworthy. First, the new augmented plant is not recommended to apply model reduction to preserve the dynamic of **D** matrix approximation. We can thus get better performance which is validated in experiments. Second, using higher orders can result in accurate fits to the data during *musynfit* operation. However, it also results in the increased dimension of the scaled open-loop interconnection, slower speed of *hinfsyn* process, and an increased order of resultant controller. After two or three *D–K* iterations, a satisfactory μ-synthesized controller is obtained. The μ-plot of the new closed-loop transfer matrix is illustrated in Fig. 12(b) and the values of μ are less than 1 within the control bandwidth, which indicates that robust performance has been achieved. The controller is then implemented to the duct ANC system and the result shown in Fig. 13(a) reveals that the total noise attenuation 7.27 dB is obtained and is comparable to the experiment results in the structure without considering the plant uncertainty.

As a benchmark test, the commonly used method for the duct ANC problem, FULMS algorithm, is compared to the proposed techniques. The details of this method can be found in Ref. [3] and are omitted here for brevity. Both the orders of the numerator and the denominator of the IIR filter used in FULMS method are 30. Total attenuation within the band 250–650 Hz is

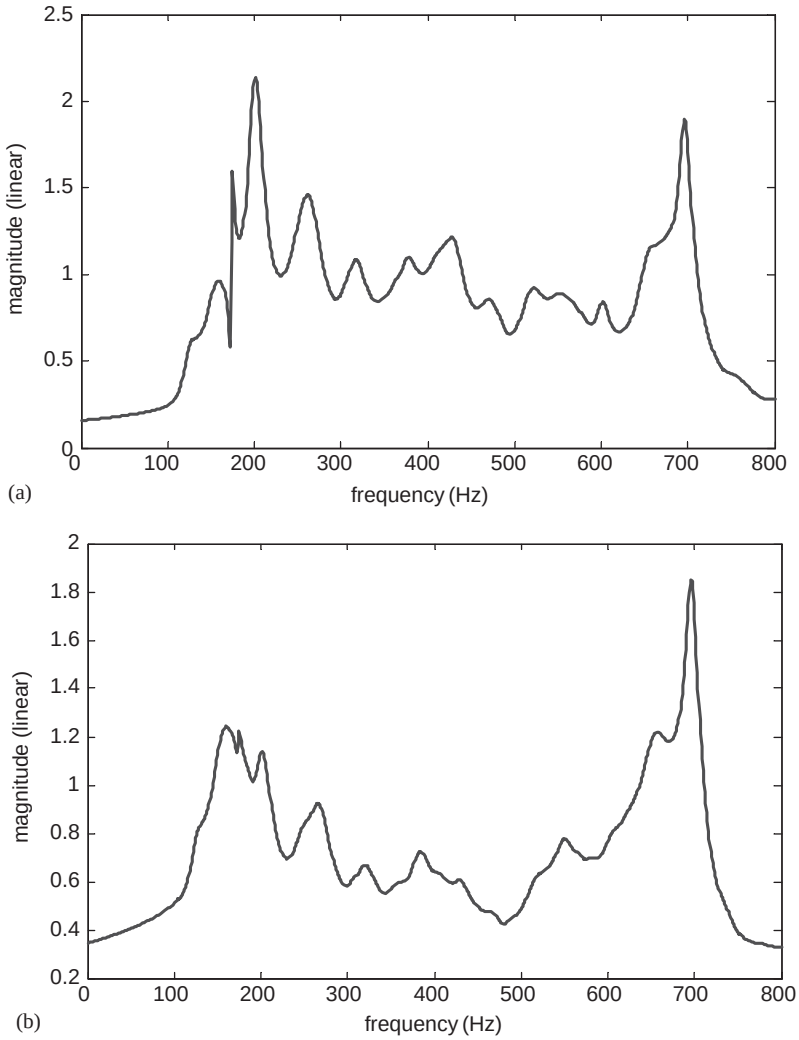

Fig. 12. μ-plots of (a) H_∞ controller and (b) μ-synthesis controller.

found to be 4.5 dB as shown in Fig. 13(b). Due to the eigenvalue spread problem and the local minimum problem, the noise reduction could only reach around 560 Hz.

Detailed comparison and all the results discussed above are summarized in Table 1. Three categories are listed in Table 1. The first one is for the control structure without considering uncertainty in which the H_2 and H_∞ controllers are implemented. In the second category, the H_∞ and μ-synthesis controllers are used in the control structure with uncertainty considered. Finally, the widely used FULMS algorithm is included as the third case. It can be observed in the results that the proposed μ-synthesis controller yields the best performance within control bandwidth. Furthermore, robust stability and robust performance are achieved within a specified, bounded uncertainty set.

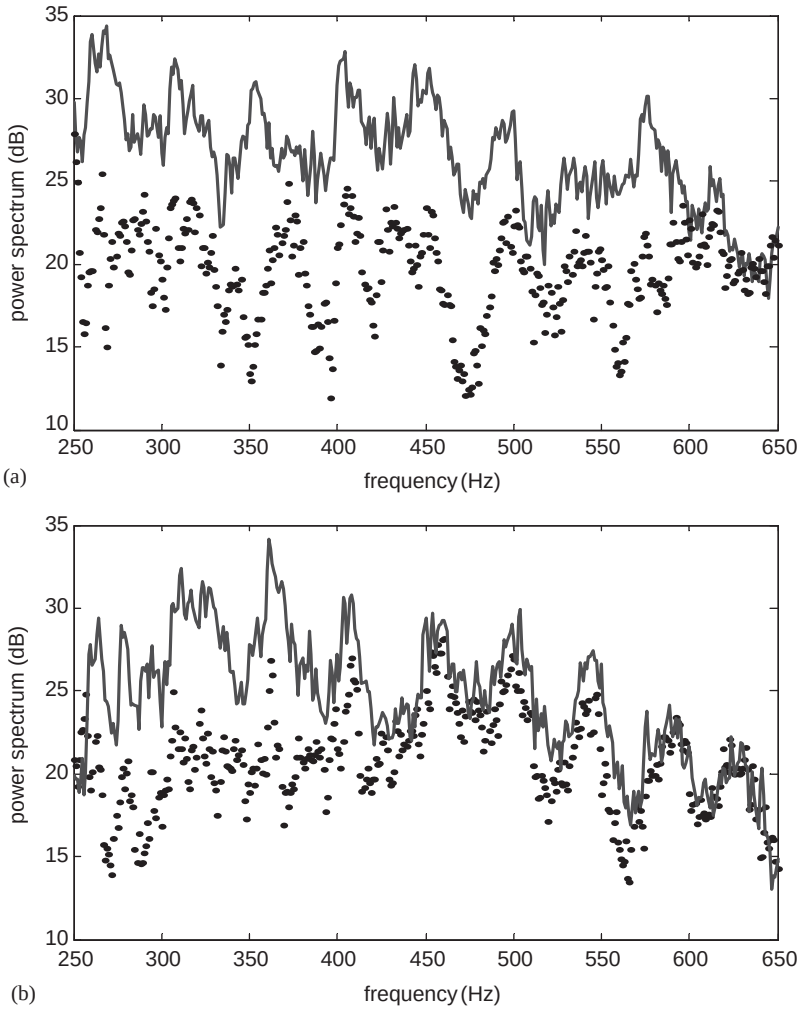

Fig. 13. Active control results of the feedforward controllers. Noise reduction using (a) μ-synthesis controller for interconnected structure in Fig. 8; (b) FULMS controller. ——, control off; ……, control on.

5. Conclusions

This paper presents a spatially feedforward design for active control of noise in a duct. The μ-synthesis techniques are employed to deal with this problem in robust fashion. Based on a nominal structural model and uncertainty description, a set of uncertainty models in which the physical system is assumed to reside are developed. Using the structured singular value framework, a controller calculated using μ-synthesis is implemented via D–K iteration for noise suppression.

To summarize, this research has two outcomes. First, it has been shown in the experiments that the controller obtained from μ-synthesis ensures robust stability and robust performance for the

Table 1
Comparison of ANC methods

Items	Algorithm				
	H_2	H_∞	H_∞	μ-synthesis	FULMS
Uncertainty considered	No	No	Yes	Yes	Yes
Control bandwidth (Hz)	250–650	250–650	250–650	250–650	250–650
Tap or order length	256	256	256	256	30
Maximal attenuation (dB)	24.2	24.4	21.5	25.8	23.1
Total band attenuation (dB)	7.17	6.77	4.37	7.27	4.5
Robust stability	No	No	Yes	Yes	No
Robust performance	No	No	No	Yes	No

duct ANC problem. In addition, it is revealed that H_∞ control is conservative, compared to μ-synthesis control when uncertainty is taken into consideration. On the other hand, although the adaptive filter using FULMS algorithm could achieve some performance in the feedforward problem, it is prone to stability problems and thus could not guarantee robust performance. Secondly, instead of theoretically working on μ-synthesis, the procedures involved in the analysis and implementation phases of the robust controller are presented in detail. Experimental verifications of the proposed ANC system were conducted for a duct problem. In particular, technical issues such as how to choose the plant uncertainty model and to form the interconnected structure for control design are addressed. From the experimental results it is clear that that the theory of μ-synthesis procedures provides a realizable robust controller to deal with the broadband duct ANC problem.

In spite of the preliminary results, the μ-synthesis controller is a fixed controller that may not be able to accommodate excessive plant perturbations such as large temperature variations in a muffler. It is reported in Eriksson's work [21] that an adaptive controller with on-line plant modelling is capable of tracking such plant variations. From the same perspective, combination of the fixed and the adaptive controllers may make it possible to improve the robustness and thus will be explored in a future study.

Acknowledgements

The work was supported by the National Science Council in Taiwan, Republic of China, under the project number NSC 87-2212-E009-022.

References

[1] R.H. Hall, W.B. Ferren, R.J. Bernhard, Active Control of Noise and Vibration, ASME, New York, 1990, pp. 143–152.

[2] J.C. Burgess, Active adaptive sound control in a duct: a computer simulation, Journal of the Acoustical Society of America 70 (1981) 715–726.

[3] L.J. Eriksson, Development of the filter-u algorithm for active noise control, Journal of the Acoustical Society of America 89 (1990) 257–265.
[4] F. Orduna-Bustamante, P.A. Nelson, An adaptive controller for the active absorption of sound, Journal of the Acoustical Society of America 91 (1992) 2740–2747.
[5] V. Eghtesadi, H.G. Leventhall, Active attenuation of noise: the monopole system, Journal of the Acoustical Society of America 71 (1982) 608–611.
[6] J. Hong, J.C. Akers, R. Venugopal, M.N. Lee, A.G. Sparks, P.D. Washabaugh, D.S. Bernstein, Modeling, identification, and feedback control of noise in an acoustic duct, IEEE Transactions on Control System Technology 4 (1996) 283–291.
[7] Z. Wu, V.K. Varadan, V.V. Varadan, Time–domain analysis and synthesis of active noise control systems in ducts, Journal of the Acoustical Society of America 101 (1997) 1502–1511.
[8] J.C. Carmona, V.M. Alvarado, Active noise control of a duct using robust control theory, IEEE Transactions on Control System Technology 8 (2000) 930–938.
[9] M.R. Bai, T.Y. Wu, Study of the acoustic feedback problem of active noise control by using the l_1 and l_2 vector space optimization approaches, Journal of the Acoustical Society of America 102 (1997) 1004–1012.
[10] M.R. Bai, H.P. Chen, Development of a feedforward active noise control system by using the H_2 and H_∞ model matching principle, Journal of Sound and Vibration 201 (1997) 189–204.
[11] J.S. Hu, Active noise cancellation in ducts using internal model-based control algorithms, IEEE Transactions on Control Systems Technology 4 (1996) 163–170.
[12] M.R. Bai, H.H. Lin, Comparison of active noise control structures in the presence of acoustical feedback by using the H_∞ synthesis technique, Journal of Sound and Vibration 206 (1997) 453–471.
[13] M.R. Bai, H.H. Lin, Plant uncertainty analysis in a duct active noise control problem by using the H_∞ theory, Journal of the Acoustical Society of America 104 (1998) 237–247.
[14] J.C. Doyle, K. Zhou, Essentials of Robust Control, Prentice-Hall, Englewood Cliffs, NJ, 1998.
[15] K. Glover, J. Doyle, State-space formulate for all stabilizing controllers that satisfy an H_∞ norm bound and relations to risk sensitivity, System and Control Letters 11 (1988) 167–172.
[16] J.C. Doyle, K. Glover, P.P. Khargonehar, B.A. Francis, State-space solution to standard H_2 and H_∞ control problems, IEEE Transactions on Automatic Control 34 (8) (1989) 831–847.
[17] G.J. Balas, J.C. Doyle, K. Glover, A. Packard, R. Smith, Matab μ-analysis and Synthesis Toolbox, The MathWorks, Inc., Natick, MA, 1994.
[18] G.J. Balas, J.C. Doyle, A. Packard, Linear multivariable robust control with a μ-perspective, American Society of Mechanical Engineers Journal of Dynamic Systems, Measurement and Control 115 (1993) 426–438.
[19] J.C. Doyle, B.A. Francis, A.R. Tannenbaum, Feedback Control Theory, Maxwell Communication Group, New York, 1992.
[20] A. Grace, A.J. Laub, J.N. Little, C.M. Thompson, Matlab Control System Toolbox, The MathWorks, Inc., Natick, MA, 1999.
[21] L.J. Eriksson, M.C. Allie, Use of random noise for on-line transducer modeling in an adaptive active attenuation system, Journal of the Acoustical Society of America 85 (1989) 797–802.